Adsorption of Organic Acids on Blast Furnace Sludge

A. Radjenovic* **and J. Malina**
University of Zagreb, Faculty of Metallurgy,
Aleja narodnih heroja 3, 44 000 Sisak, Croatia

Original scientific paper
Received: February 8, 2008
Accepted: September 25, 2008

This paper describes the adsorption of two organic (acetic and citric) acids on the blast furnace sludge, a representative by-product of the steelmaking industry.

By PIXE, XRD, BET and SEM methods, it was shown that blast furnace sludge is a complex heterogeneous material with a specific surface area of $s = 31.46$ m^2 g^{-1}, composed mainly of amorphous phase ($w = 76.2$ %), calcite ($w = 9.9$ %), magnetite ($w = 6.3$ %) and kaolinite ($w = 2.2$ %). Chemically, blast furnace sludge is dominated by O ($w = 42.23$ %) and C ($w = 31.74$ %).

The adsorption process is analyzed using the theories of Freundlich and Langmuir. The experimental data were better fitted to the Langmuir isotherm. The negative Gibbs energy values indicate the spontaneous nature of adsorption. After adsorption the surface image changes in the BFS were observed, and BET surface area increased when acetic acid was adsorbed. Contrarily, blast furnace sludge became almost non-porous in the case of citric acid adsorption and BET surface area decreased significantly.

Key words:
Blast furnace sludge, organic acids, adsorption

Introduction

It is known that application of adsorbents is strongly influenced by their surface properties. The performance of materials as adsorbents is determined by their both texture and surface chemistry. The texture may be adapted by adequate choice of the activation procedure. The nature and concentrations of surface functional groups may be modified by suitable thermal or chemical treatments. Surface modification can be performed by adsorbing foreign organic compounds on the surface of adsorbents.[1,2]

In natural water systems, organic acids on solid surfaces can bind heavy metal ions by forming complexes. This process inhibits the retention of heavy metals by sediments and favors their transportation in aquatic environments. Citric acid and acetic acid are often cited as organic ligands involved in the adsorption process in soil chemistry. Their presence in soil systems might be expected to have a significant effect on the adsorption of metal ions to mineral particles. Kubicki *et al.*[3] investigated the bonding of salicylic acid adsorbed onto the clay mineral illite. Adsorption of citric acid onto both kaolinite and goethite by means of batch experiments was investigated by Redden and co-workers.[4] Du *et al.*[5] conducted various experiments to study the adsorption of fulvic acid on illite surfaces and interaction between illite-fulvic acid system with copper (II) ions. Lacković *et al.* investigated the adsorption of Cd(II) and citric acid separately onto goethite, kaolinite and illite.[6] The same authors suggest modeling the adsorption of Cd(II) onto kaolinite and illite in the presence of citric acid.[7] Furnier and co-workers showed that acetic acid enhanced lead adsorption onto kaolinite.[8]

In recent years, research efforts have been directed towards the use of industrial waste or by-products as adsorbent material in the attempt to minimize processing costs. The steelmaking industry by-products were investigated as effective adsorbents and used for the removal of metal ions and dyes.[9–13]

Blast furnace sludge (BFS) is a by-product of the steelmaking industry. The gases generated during the manufacture of pig iron carry a dust load which is cleaned before their release in the atmosphere. The coarse particles in the exhaust gases are removed by passing the gases through a large lined chamber. The velocity of gases is reduced to allow the settling of dust load and the waste material is collected as blast-furnace dust. The finer particles, which remain in the gas, are removed in wet scrubbers; the waste material collected here is BFS. From the wastes in steel plants, the slag is produced in the largest amount while dust and sludge occurs in lesser amounts.

Due to the lack of literature data on BFS interaction with organic acids, the aim of this work was to study adsorption of acetic and citric acid onto the waste blast furnace sludge collected from an aban-

*Corresponding author: E-mail: radenova@simet.hr

doned sludge landfill. Both acetic and citric acid are biodegradable and widely used in the food and pharmaceutical industries. The key idea was to see the influence of organic adsorbates on the texture and surface characteristics of blast furnace sludge after adsorption process. This work should be considered the first, but important step toward further application of BFS modified by acetic/citric acid adsorption.

Experimental

Materials

The original BFS, provided by a Croatian Iron & Steelmaking Company, was dried at θ = 105 °C for 4 h to yield a powder of a particle diameter less than d_p = 56 μm.

Two organic acids (mono and tricarboxylic acid) were used: acetic acid (H_3C–COOH) which is characterized by one pK (4.75), and citric acid (HOOC–CH_2–COH–COOH–CH_2–COOH) characterized by three pK (pK_1 = 3.128, pK_2 = 4.761, pK_3 = 6.396).[14]

Methods for characterization of the BFS

The chemical composition of the ground sample was determined by Proton Induced X-ray Emission (PIXE) and Rutherford Backscattering Spectrometry (RBS) techniques. PIXE quantification was done using GUPIX, and RBS determinations used SIMNRA software.[15]

Conventional X-ray diffraction (XRD) analysis yield qualitative mineralogical composition. Accurate quantitative composition of BFS is achieved by Rietveld refinement of XRD analyses.[16] Qualitative overview analysis indicated large amounts of XRD amorphous material in BFS. The quantification of XRD amorphous phases was done following the procedure in which internal quantification standard was mixed with the sample. Subsequently, the crystalline phases were quantified by Rietveld refinement. This yields absolute portions of all crystalline phases calculated. Based on the known addition of the internal standard, absolute XRD crystalline phase contents can be calculated. The amount of XRD amorphous phases is given by the difference between 100 %, and the sum of all crystalline phases quantified above.

In this study, ZnO was used as the internal standard. ZnO was mixed with the samples to give a proportion of w = 10 %. The mixture was homogenized by hand in an agate mortar for about 30 min. Mineralogical composition of these mixtures was determined by XRD analysis using a Philips PW 1710 difractometer with Cu K_α radiation.

Batch adsorption

The adsorption of organic acids on the BFS was carried out via a batch technique. Accordingly, 100 mL solutions of known concentration of acids (in range: c_i = 0.05–0.35 mol L^{-1}) was added to reagent bottles with 1 g of dry BFS. The suspension was shaken for a period of 30 min. Although the experiments were performed within the time intervals from 0–48 hours, equilibrium was established after 1 hour. The initial pH value of solutions varied in the range 2.01–3.53 depending on the starting concentration of acids. After adsorption process was completed, the measured pH values were 2.9–4.1. Acid concentrations before and after equilibrium were determined by titrating with a 0.1 mol L^{-1} NaOH solution and phenolphthalein as indicator.

The samples were then washed with deionized water until no turbidity could be observed when a 0.1 mol L^{-1} lead nitrate solution was added to the washed liquid.

Experiments were performed at a fixed temperature of θ = 20 °C and sludge mass concentration of γ = 10 g L^{-1}.

All chemicals used in this study were analytical grade (Merck), including high purity ion-free water.

The experiments were carried out in triplicate and the average results presented.

Surface properties

The surface image of BFS samples was visualized by scanning electron microscopy (SEM) using a JEOL JXA, 50A microscope.

The following physical characteristics of BFS were also determined: surface area and average pore diameter. The surface area was calculated by the Brunauer-Emmett-Teller (BET) method. Before adsorption isotherms were obtained, the BFS samples were heated (at θ = 50 °C) and evacuated under $p = 666.5 \cdot 10^{-3}$ Pa pressure in order to remove any contaminants as well as moisture that might be present on the surface. Measurements were performed by Micromeritics ASAP 2000 instrument.

Results and discussion

Characterization of the blast furnace sludge

Chemical composition of the BFS is shown in Table 1. It can be seen that the BFS is dominated by O (w = 42.33 %) and C (w = 31.74 %). The other elements come from the blast furnace operation, i.e. from iron ores, metallurgical coke and fluxing agents. The air carries coke and fluxing agent's particles over iron ores into the top gas, so that the

Table 1 – *Chemical composition of blast furnace sludge*

Element	Mass fraction *w*/%	Element	Mass fraction *w*/%
O	42.23	Pb	0.99
C	31.74	K	0.66
Si	6.00	Mn	0.66
Zn	4.52	S	0.62
Na	3.00	P	0.14
Al	3.00	Cl	0.05
Fe	2.90	Ti	0.05
Ca	2.30	Cu	0.01
Mg	1.00		

chemical composition of BFS depends on the process of pig-iron production.

The accurate mineralogical composition data (Table 2) are also important in order to clarify the environmental significance of the BFS. The obtained results indicated a large amount of XRD amorphous phase (w = 76.2 %). These phases are essentially composed of turbostratically disordered coke. Moreover, less crystalline oxides or hydroxides of metals such as Zn, Al, Pb, Fe, as well as drops of melted silica could be present in amorphous compounds.[17]

Table 2 – *Mineralogical composition of blast furnace sludge*

Compound	Formula	Mass fraction *w*/%
X-ray amorphous		76.2
Calcite	$CaCO_3$	9.9
Magnetite	Fe_3O_4	6.3
Kaolinite	$Al_2Si_2O_5(OH)_4$	2.2
Smithsonite	$ZnCO_3$	2.1
Dolomite	$Ca,Mg(CO_3)_2$	1.6
α-Quartz	α-SiO_2	1.1
α-Hematite	α-Fe_2O_3	0.4
α-Elemental iron	α-Fe	0.2

The mineralogical composition can be partially related to the material used in the blast furnace process. While fluxing agents are the source of both calcite and dolomite, quartz and kaolinite originate mainly from ash-containing coke; iron ores are the source of magnetite and hematite.

Batch adsorption

The variation of the acids fractions adsorbed during the equilibration is shown in Fig. 1. The mole fraction of citric acid (CA) and acetic acid (HAc) adsorbed at any time, $\chi(t)$ was calculated using the following relation:[18]

$$\chi(t) = \frac{c_i - c_t}{c_i} \quad (1)$$

where: $\chi(t)$ is the mole fraction of acids adsorbed at time t on BFS; c_i is the initial concentration of acid in solution, mol L^{-1} and c_t is the concentration of acid in solution at time t, mol L^{-1}.

As shown in Fig. 1, the adsorption of acids on BFS increases with increasing contact time, especially after 30 minutes for c_i = 0.05 mol L^{-1}. For c_i = 0.25 mol L^{-1} this effect is less noticeable. It can be observed that the adsorption kinetics is similar for both BFS-HAc and BFS-CA system. Obviously, the adsorption takes place in two distinct steps, a relatively slow one followed by a faster one. The slow adsorption is explained by the diffusion into the pores of BFS. Based on the theory, kinetics of adsorption on a heterogeneous solid surface is determined by the following stages: (1) diffusion of molecules from the bulk phase towards the interface space (so-called external diffusion); (2) diffusion of molecules inside the pores (internal diffu-

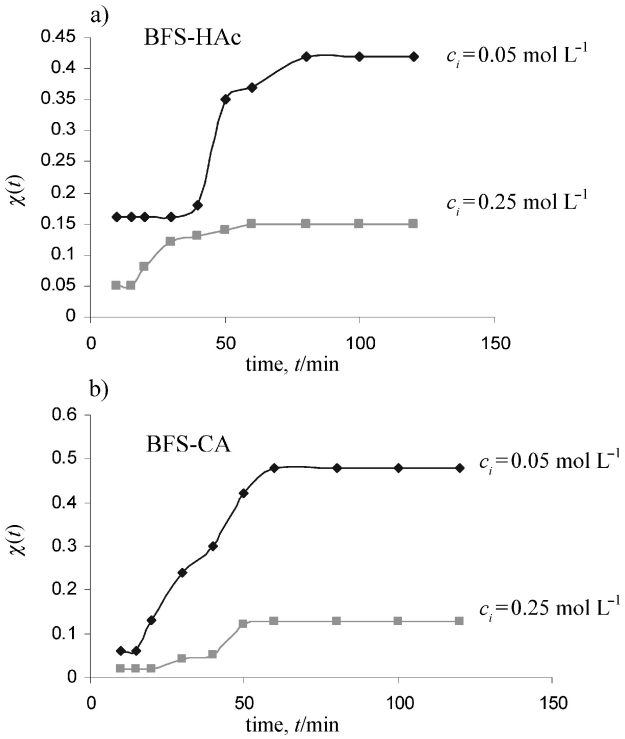

Fig. 1 – *Mole fraction, $\chi(t)$ of: a) acetic acid and b) citric acid adsorbed on BFS against time for two different initial concentrations of acids (concentration of BFS γ = 10 g L^{-1}; temperature θ = 20 °C)*

sion); (3) diffusion of molecules in the surface phase (surface diffusion) and (4) adsorption/desorption elementary process.[19]

The adsorption isotherm indicates how the adsorbate molecules distribute between the liquid phase and the solid phase when the adsorption process reaches an equilibrium state. The analysis of the equilibrium data by fitting them to isotherm models is an important step to find the suitable model that describes the adsorption process. Hence, the amount of both HAc and CA adsorbed per mass unit of BFS (adsorption capacity, q_e, mol g^{-1}) was calculated according to the formula:

$$q_e = (c_i - c_e) \cdot \frac{V}{m} \tag{2}$$

where c_i and c_e are initial and equilibrium concentrations of acids (mol L^{-1}), V is the solution volume (L) and m is the mass of adsorbent (BFS, g). The results are shown in Fig. 2.

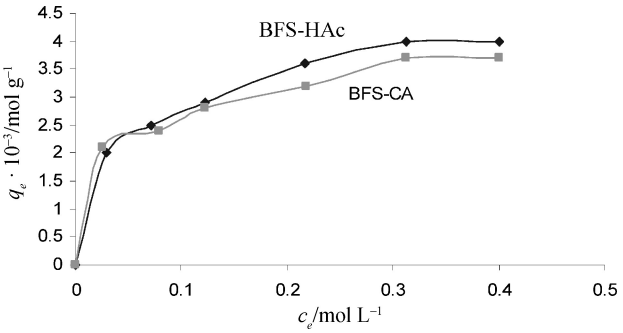

F i g . 2 – *Amount of HAc and CA adsorbed per unit mass of BFS depending on equilibrium concentration of acids*

It can be concluded that there was no significant difference between the adsorption capacity for HAc and CA. Maximum adsorption capacity obtained for HAc is q_e (HAc) = 0.004 mol g^{-1} while for CA is q_e (CA) = 0.0037 mol g^{-1}.

For the interpretation of adsorption equilibrium data, the most widely used Langmuir and Freundlich isotherms were applied. The Langmuir model assumes that adsorption takes place on the homogeneous surface of the adsorbent and at saturation a monolayer is formed, while the Freundlich expression is an empirical equation based on adsorption on a heterogeneous surface. The Langmuir isotherm based on the ideal monolayer adsorbed model is applicable to most real adsorption systems that include structurally (high porous) heterogeneous solids.[19]

Accordingly, in the system BFS-organic acid, the Langmuir isotherm used to describe the adsorption process is:

$$q_e = \frac{q_{\max} K_L c_e}{1 + K_L c_e} \tag{3}$$

where q_e and c_e are the same as in eq. (2), $q_{\max}$ is the maximum adsorption capacity and K_L is constant related to adsorption intensity. The constants $q_{\max}$ and K_L can be determined from a form of eq. (3), represented by:

$$\frac{c_e}{q_e} = \frac{1}{q_{\max} K_L} + \frac{c_e}{q_{\max}} \tag{4}$$

The Freundlich isotherm is an empirical equation that can be used for non-ideal sorption and is commonly presented as:

$$q_e = K_F c_e^{1/n} \tag{5}$$

K_F is the Freundlich adsorption constant and *1/n* is related to adsorption intensity. It is expressed as:

$$\ln q_e = \ln K_F + \frac{1}{n} \ln c_e \tag{6}$$

The obtained data fit the linear relationship of both Freundlich (Fig. 3) and Langmuir (Fig. 4) ishoterm well.

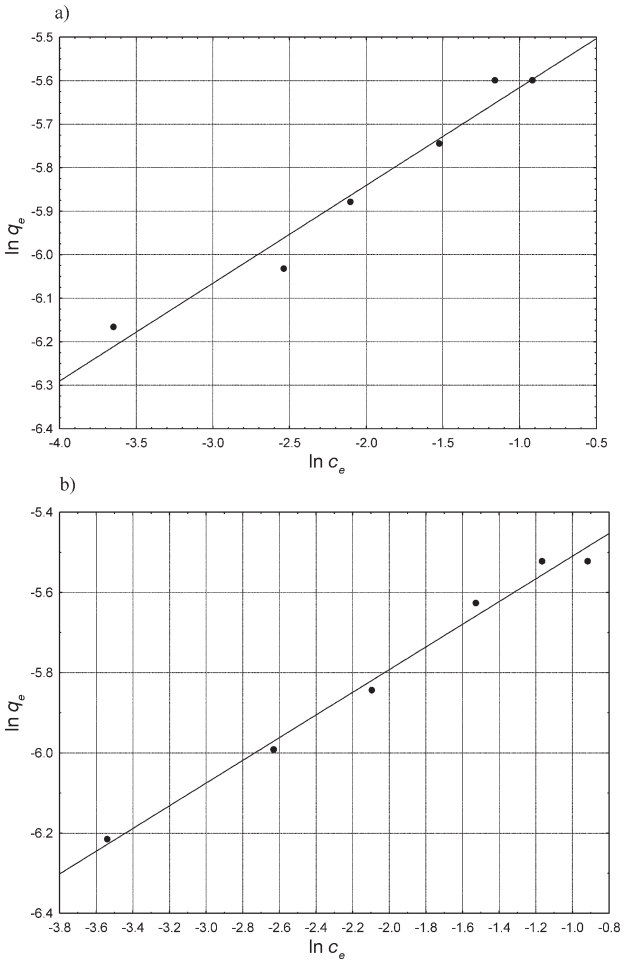

F i g . 3 – *Freundlich adsorption isotherm of: a) citric and b) acetic acid on BFS*

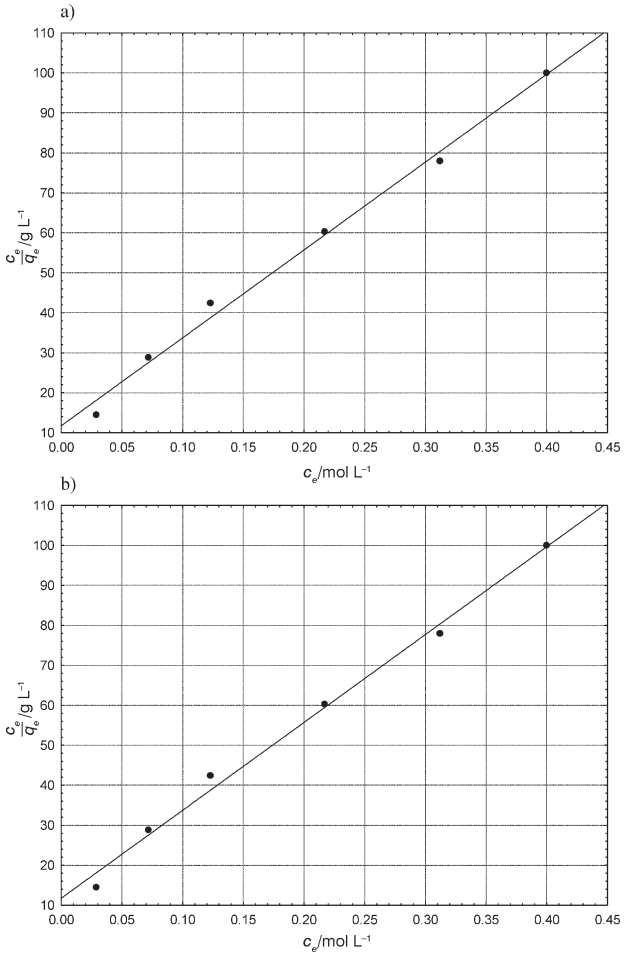

F i g . 4 – *Langmuir adsorption isotherm of: a) citric and b) acetic acid on BFS*

The values of Langmuir and Freundlich constants and correlation coefficients *(R^2)* were determined and shown in Table 3. The correlation coefficient *(R^2)* values indicated that, generally, experimental data were well fitted to the Langmuir equation. Namely, the R^2 value for HAc adsorption on BFS is 0.9506; for CA adsorption on BFS R^2 value is 0.9416. The maximum adsorption capacities are: q_{max} = 4.53 mmol g^{-1} for HAc and q_{max} = 4.19 mmol g^{-1} for CA.

The minimum correlation coefficient *(R^2* = 0.8460) is obtained using the Freundlich equation for HAc adsorption on BFS, while the greatest R^2 value (0.9520) is obtained using the Freundlich equation for CA adsorption on BFS. Values of q_{max} and K_L for CA as compared to HAc confirm the affinity of BFS for both acids, but this one is not similar, there is a difference.

The experimental results fit the Langmuir model (isotherm) well for both studied acids (R^2 > 0.94). However, Freundlich isotherm is only acceptable to quantify the citric acid adsorption on BFS.

Standard Gibbs energy for the process is calculated as: $\Delta G = - R\ T\ \ln K_L$. The negative Gibbs energy values (Table 3) indicate the feasibility of the process and the spontaneous nature of both HAc and CA adsorption on investigated BFS.

Surface properties

A fundamentally important feature of adsorbents is their high porosity and usually high surface area. That is why their most important characteristics deal with total pore volumes, pore size distribution over the pore diameter and the specific surface area. The adsorption capacities can be related to surface area properties of BFS as follows. BET specific surface area of BFS was s = 31.46 m^2 g^{-1} and average pore diameter determined by BET method was d = 17.88 nm. Total pore volume (1.7–300 nm pore diameter) was v = 0.157 cm^3 g^{-1}. According to average pore diameter value, the BFS may be considered mesoporous material.

BET surface area of BFS after CA adsorption has a very low value (s = 3.31 m^2 g^{-1}). The sample was nearly non-porous. Contrarily, in the case of HAc adsorption, BET specific surface area was s = 35.55 m^2 g^{-1}, and the average pore diameter for this sample was 16.44 nm. Total pore volume (1.7–300 nm pore size) was v = 0.165 cm^3 g^{-1}. This difference in BET surface characteristics of investigated samples is also confirmed by SEM method.

SEM micrographs of the BFS surface are shown in Fig. 5. Scanning electron microscopy enables the direct observation of any surface morphology changes in the BFS that would have occurred due to the acid adsorption. Clearly visible are accumula-

T a b l e 3 – *Adsorption isotherm constants for system BFS-organic acid*

Adsorbate	Langmuir constants				Freundlich constants		
	$\frac{q_{max} \cdot 10^3}{\text{mol g}^{-1}}$	$\frac{K_L}{\text{L mol}^{-1}}$	R^2	$\frac{\Delta G}{\text{kJ mol}^{-1}}$	$\frac{K_F}{(\text{mol g}^{-1})/(\text{L mol}^{-1})^{1/n}}$	n	R^2
HAc	4.53	18.236	0.9506	–7.072	0.0053	3.66	0.8460
CA	4.19	17.644	0.9416	–6.992	1.608	5.12	0.9520

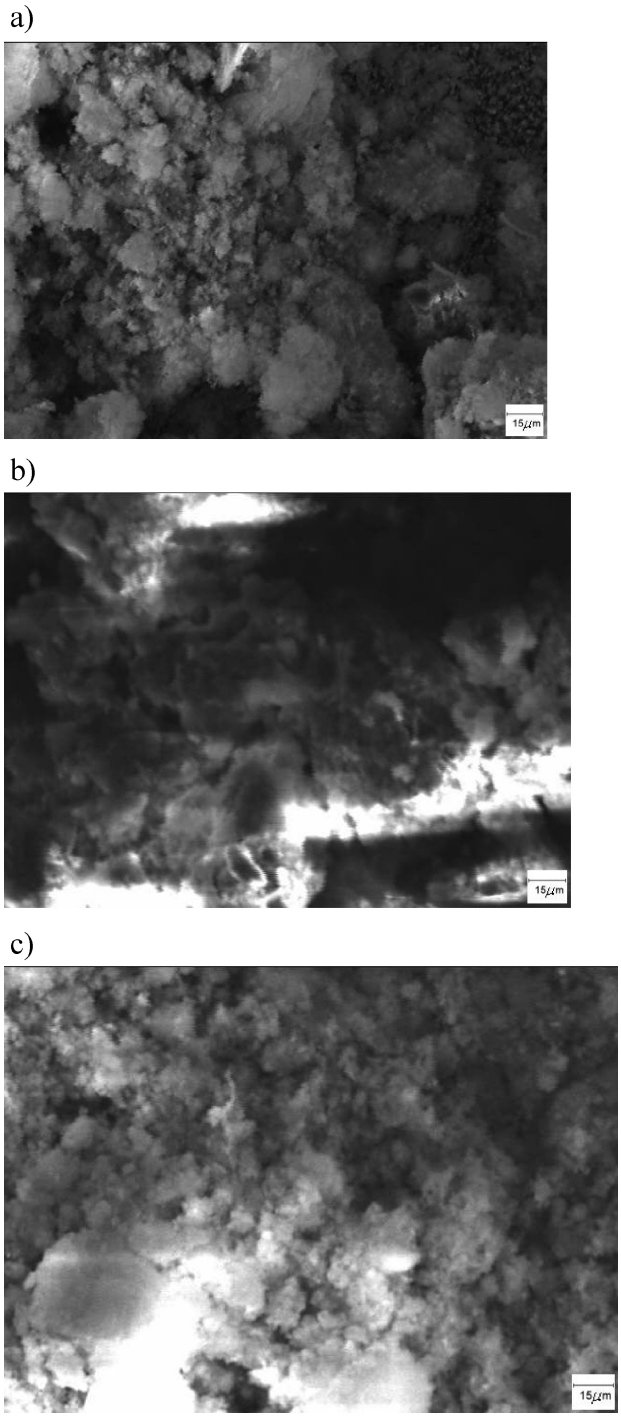

Fig. 5 – *SEM micrographs of the BFS surface: a) before adsorption; b) after CA adsorption and c) after HAc adsorption;* c_i *(HAc) =* c_i *(CA) = 0.05 mol* L^{-1}*, contact time, t = 1 h*

tions and deposits of CA and HAc adsorbed on BFS surface. Different pore diameter is also observed as change in morphology of samples. The heterogeneity in the surface or pores of the BF sludge will play a role in acid adsorption. Thus, BFS possess a complex porous structure, which consists of pores of different sizes and shapes. For such mesoporous material, the layer-by-layer adsorption mechanism could be supposed as effective.[19]

According to mineralogical composition and the performed chemical analyses, the investigated BFS contained mainly oxides and carbon (Tables 1 and 2). Literature data indicate that BFS with such composition could be considered an effective adsorbent.[20,21] This can be related to its high iron oxide and carbon mass fraction, since both contain oxygenated surface functional groups. Oxides will always be the most important minerals for carboxylic acids adsorption in natural systems. Namely, modeling of mineral systems suggests that adsorption occurs onto surface hydroxyl groups. Citric acid adsorption onto kaolinite, goethite and illite, was modeled with outer-sphere complexation to the variable charge edge groups.[6,7,22,23] Additionally, the adsorption behavior of the studied adsorbates on silica surface should also be mentioned.[24,25] It is known that silica surface is generally embedded with hydroxyl groups, and hence considered to have a negatively charged surface prone to adsorption of deficient species like CA and HAc.

Conclusion

The use of blast furnace sludge as an adsorbent for the acetic and citric acid from aqueous solutions was evaluated.

The Langmuir and Freundlich isotherms were used to determine the adsorption capacity of both acetic and citric acid. The experimental data were better fitted to the Langmuir equation ($R^2 > 0.94$). The negative Gibbs energy values indicated the spontaneous nature of adsorption.

It was shown that the surface morphology of BFS and BET surface characteristics were changed under the influence of HAc and CA adsorption.

Chemical composition reflecting the pig-iron production technology dominates the BFS adsorption characteristics. While amorphous phase (mostly carbon) content provides the beneficial BET specific surface area, different oxides detected could be responsible for the preferential adsorption of organic acids tested.

The adsorption of CA and HAc on BFS is shown to be an adequate activation procedure for its surface modification. Modified BFS with enhanced surface activity (via functional carboxylic groups) could be considered a potential adsorbent for further application such as wastewater treatment.

ACKNOWLEDGEMENT

This work was supported by the Ministry of Science, Education and Sports of the Republic of Croatia, under the project 124-1241565-1524.

Nomenclature

c_e – equilibrium concentration of adsorbate, mol L^{-1}
c_i – initial concentration of adsorbate in solution, mol L^{-1}
c_t – concentration of adsorbate in solution at time, mol L^{-1}
d_p – particle diameter, μm
K_F – constant of Freundlich isotherm, $(mol\ g^{-1})/(L\ mol^{-1})^{1/n}$
K_L – constant of Langmuir isotherm, L mol^{-1}
m – mass of adsorbent, g
n – exponent in Freundlich isotherm
p – pressure, Pa
q_e – equilibrium adsorption capacity of adsorbent, mol g^{-1}
q_{max} – maximum adsorption capacity of adsorbent, mol g^{-1}
R^2 – correlation coefficient
s – specific surface area, $m^2\ g^{-1}$
t – time, min
V – volume of solution, L
v – specific volume, $cm^3\ g^{-1}$
w – mass fraction, %
$\chi(t)$ – mole fraction of adsorbate adsorbed at any time
ΔG – Gibbs free energy, kJ mol^{-1}
γ – mass concentration, g L^{-1}
θ – temperature, °C

References

1. *Figueireds, J. L., Pereria, M. F. R., Freitas, M. M. A., Orfao, J. J. H.*, Carbon **37** (1999) 1379.
2. *Rađenović, A., Malina, J., Slokar, Lj.,* Proceedings of the 2nd Croatian Congress on Microscopy, *Gajović, S.* (Ed.), Croatian Society for Electron Microscopy, Topusko, (2006) 262.
3. *Kubicki, J. D., Schroeter, M. J., Itoh, Nguyen, B. N., Apitz, S. E.*, Geochim. Cosmochim. Acta **63** (1999) 2709.
4. *Redden, G. D., Li, J.,* in *Jenne E. A.,* (Ed.), Adsorption of metals by Geomedia, Academic Press, San Diego, 1998.
5. *Du, Q., Sun, Z., Forsling, W., Tang, H.*, Wat. Res. **33** (1999) 693.
6. *Lacković, K., Johnson, B. B., Angove, M. J., Wells, J. D.*, J. Colloid. Interface Sci. **267** (2003) 49.
7. *Lacković, K., Wells, J. D., Johnson, B. B., Angove, M. J.*, J. Colloid. Interface Sci. **270** (2004) 86.
8. *Furnier, P., Oelkers, E. H., Gout, R.*, Mineral. Mag. A **62** (1998) 464.
9. *Martin, M. I., Lopez, F. A., Perez, C., Lopez-Delgado, A., Alguacil, F. J.*, J. Chem. Technol. Biotechnol. **80** (2005) 1223.
10. *Lopez-Delgado, A., Perez, C., Lopez, F. A.*, Wat. Res. **32** (1998) 989.
11. *Dimitrova, S. V.,* Wat. Res. **30** (1996) 228.
12. *Jain, A. K., Gupta, V. K., Bhatnagar, Suhas, A.*, J. Hazard. Mater. **B101** (2003) 31.
13. *Gupta, V. K.,* Ind. Eng. Chem. Res. **37** (1998) 192.
14. *Dean, J. A.,* Lange's Handbook of Chemistry, McGraw-Hill Book Company, New York, 1985, pp. 5–18 and 5–28.
15. *Bogovac, M., Bogdanović, I., Fazinić, S., Jakšić, M., Wilhelm, W.*, Nucl. Instr. and Meth. **B89** (1994) 219.
16. *Young, R. A.,* The Rietveld Method, Oxford University Press, Oxford, 1993.
17. *Mansfeldt, T., Dohrmann, R.,* Environ. Sci. Technol. **38** (2004) 5977.
18. *Qadeer, R., Hanif, J.,* Carbon **32** (1994) 1433.
19. *Dabrowski, A.,* Adv. Colloid. Interface Sci. **93** (2001) 135.
20. *Lopez-Delgado, A., Perez, C., Lopez, F. A.*, Carbon **34** (1996) 423.
21. *Lopez, F. A., Perez, C., Lopez-Delgado, A. J.*, J. Mater. Sci. Lett. **15** (1996) 1310.
22. *Ali, M. A., Dzombak, D. A.,* Environ. Sci. Technol. **30** (1996) 1061.
23. *Evanko, C. R., Dzombak, D. A.,* J. Colloid. Interface Sci. **214** (1999) 189.
24. *Parida, S. K., Dash, S., Patel, S., Mishra, B. K.*, Adv. Colloid. Interface Sci. **121** (2006) 77.
25. *Bose, A., Gilpin, R. K., Jaronie, M. J.,* J. Colloid. Interface Sci. **240** (2001) 224.